Journal of
Materials Chemistry A

Accepted Manuscript

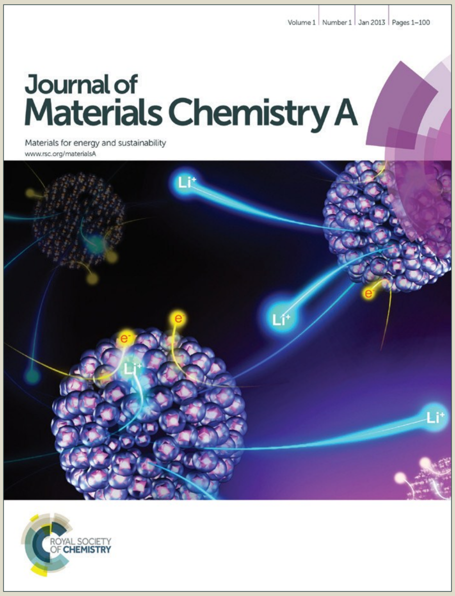

ROYAL SOCIETY OF CHEMISTRY

www.rsc.org/materialsA

# Ultrafast, high-performance, and no pretreatment extraction of uranium from seawater by both acylamide- and carboxyl-functionalized metal-organic framework

Ling Ling Wang, Feng Luo, Li Long Dang, Jian Qiang Li, Xiao Liu Wu, Shu Juan Liu, and Ming Biao Luo

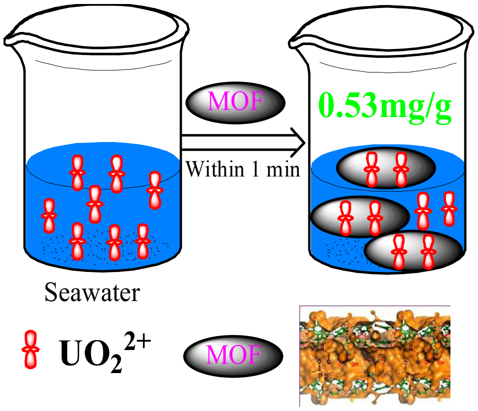

A facile method by means of MOF material is for the first time used for the extraction of U(VI) ions from seawater, giving a significant extraction efficiency of 0.53 mg/g. This method is ultra-fast within 1 min, high-performance, and no pretreatment for the material.

Journal Name RSCPublishing

ARTICLE

Cite this: DOI: 10.1039/x0xx00000x

Received 00th January 2012,
Accepted 00th January 2012

DOI: 10.1039/x0xx00000x

www.rsc.org/

# Ultrafast, high-performance, and no pretreatment extraction of uranium from seawater by both acylamide- and carboxyl-functionalized metal-organic framework

Ling Ling Wang, Feng Luo,* Li Long Dang, Jian Qiang Li, Xiao Liu Wu, Shu Juan Liu, and Ming Biao Luo

Extraction of uranium from seawater is very important for the growing crisis in energy and sustainable development, and consequently attracted enormous attention. Herein, we report the application of MOF materials in extraction of uranium from seawater. Without any pre-treatment and within one minute, this MOF material shows an one-off extraction efficiency of 0.53 mg/g from 1L artificial seawater in the concentration of 6 ppb, suggesting significant potential in extraction of uranium from seawater. This significant ability is mainly dependent on free standing carboxyl groups in the MOF channel that coordinate to $UO_2^+$ ions *via* U-O coordination bond.

## Introduction

Metal-organic frameworks (MOFs) are a class of crystalline hybrid materials in which metal ions or metal clusters are linked by various organic bridging ligands[1,2]. With the high and permanent porosity and fine-tunable pore structures, extraordinary surface areas and adjustable chemic functionality[3, 4], MOFs represent unique advantages over the material's wholly organic or inorganic porous counterparts in the last two decades. Therefore more and more researchers are becoming interested in exploring the promising application of MOFs in a variety of fields, including drug delivery, biological-imaging[5], gas adsorption/separation[6], luminescence[7], magnetic[8], catalysis[9], and so on.

On the other hand, the demand for alternative fuels is greater now than perhaps ever before because of the concerns over energy security, air quality, global warming and climate change[10]. Nuclear power as a kind of the high efficiency and clean energy are helpful for addressing the shortage of fossil fuels and concerns regarding climate change[11]. Meantime, uranium is the most important element in the development and utilization of nuclear power[12]. As it is estimated by IAEA (International Atomic Energy Agency), the total identified conventional uranium resources can only last for about 80 years[13]. Therefore, for the sustainable development of nuclear power, making the best use of the some new uranium sources at low cost is becoming more than necessary and urgent[14]. Although the concentration of uranium in seawater is low, the volume of the world's oceans is so large, approximate $5\times10^9$ km$^3$, that seawater could still provide almost limitless amounts of the metal, nearly 1000 times of the estimated terrestrial reserves[15]. So, seawater is an inexhaustible resource for uranium. In this context, it is of great significance to develop effective treatment techniques for removing uranium ions from seawater. As we all know, there are a variety of methods for the removal of uranium(VI) from aqueous solution, but most available methods may have economical and technical disadvantages, for example high cost, or high sensitivity to operational conditions, or slow reaction rate. Taking these factors into consideration, adsorption is recognized as an effective and economic method for uranium(VI) removal from wastewater and seawater[16]. To date, it has been reported that most materials which are utilized to remove uranium species are pure inorganic components[17]. Very little attention has been given to examples with fast adsorption rate and good selectivity; and it has been reported that Lin *et al.* used the MOFs (UiO-68) as sorbents to extract actinide elements from the aqueous solution for the first time.[18] This indicates that MOFs which have large pore apertures to facilitate the transport of actinide elements will be one of the best candidates for effective treatment of uranium residuals. However, there still is at an early stage referring to extraction of uranium from seawater by means of MOF materials. Herein, one MOF material with regular 1D channel decorated by both acylamide and carboxyl units is selected for the exploration of extracting uranium from seawater[19]. Notably, an one-off extraction efficiency of 0.53 mg/g from 1L artificial seawater in the concentration of 6 ppb is obtained by this MOF, suggesting unique potential aiming at extraction of uranium from seawater.

## Results and discussion

The MOF, Zn(HBTC)(L)·$(H_2O)_2$ ($H_3BTC$=1,3,5-benzenetricarboxylic acid, L=$N^4$,$N^{4'}$-di(pyridine-4-yl)biphenyl-4,4'-dicarboxamide) was synthesized by the self-assembly of $Zn(NO_3)$, $H_3BTC$, and L ligand.[19] Typically, DMF/$H_2O$ (6 mL, 5:1) solution of $Zn(NO_3)_2$, L, $H_3BTC$ in a ratio of 1:1:1 was heated at 120℃ in a Teflon reactor for 2 days, then cooled to the room temperature at 3℃/h with yield of 92% based on Zn. The phase purity is confirmed by PXRD (powder X-ray diffraction) investigation (Fig. 7). The structure is shown in Fig. 1. The MOF presents 1-D regular hexagonal channel along the *c* axis with effective aperture of ca. 4.0Å. Careful inspection of the MOF discloses that the pore wall is decorated by abundant, free standing acylamide and carboxyl groups, indicative of potential of providing additional coordination or supramolecular capability. In literature, MOFs with free standing carboxyl groups in the channel have been observed by Eddaoudi and Clet, where selective gas adsorption was established.[20]

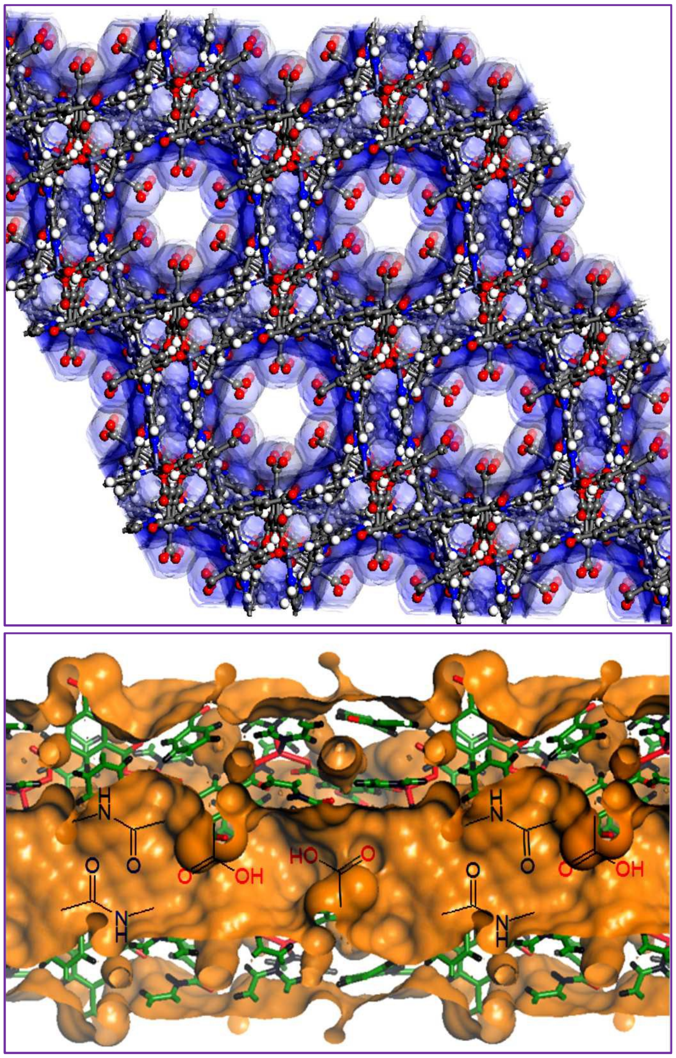

**Fig. 1** View of the 3D framework of this material with 1D channel along *c* axis and the section description of the location of both acylamide and carboxyl units.

To first evaluate the performance of U(VI) adsorption of this MOF material, a series of batch adsorption tests were carried out, such as the effects of pH, contact time, temperature, and initial concentration on U(VI) uptake. In a typical procedure, uptake experiments were performed at controlled pH (1-5) and 298K. The solution pH was adjusted to the desired value by HCl and $NH_3·H_2O$. The amount of adsorbed uranium at the equilibrium was calculated from the difference of the U concentration in the aqueous before and after the adsorption according to the equation (1):

$$q = (C_0 - C_e) \times \frac{V}{m} \qquad (1)$$

where *q* (mg/g) is the amount of U adsorbed on adsorbent; $C_0$ (mg/L) and $C_e$ (mg/L) are the initial and equilibrium concentrations of uranium in the solutions, respectively; *m* (g) is the mass of MOF material; and *V* ( L) is the volume of aqueous solution.

In general, uranium species varies over the pH range. Uranium becomes increasingly hydrolyzed and forms oligorimeric species with the increasing pH. It has been reported[21] that at pH≤4.3, uranium exist predominantly as monomeric species, $UO_2^{2+}$, and small amount as $UO_2^{2+}(OH)^+$. When pH≥5, the formation of colloidal or oligomeric species, such as $(UO_2)_2(OH)_2^{2+}$, $(UO_2)_3(OH)_5^+$, $(UO_2)_4(OH)_7^+$, $(UO_2)(OH)_7^-$, are formed. The results of pH experiments are presented in Fig. 2. We can see that Uranium adsorption is strongly dependent on pH value of the solution. The adsorption of uranium clearly increases from 55 mg/g to 92 mg/g with an increase in pH of the solution from 1.0 to 2.0 and then slightly decreases to 85 mg/g at pH=5. Then, the optimum pH=2 was selected for succedent research.

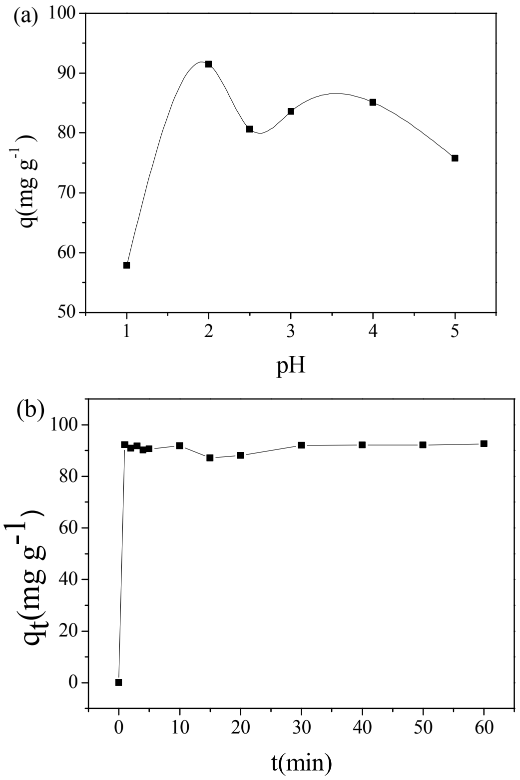

**Fig. 2** (a) Effect of solution pH on the U(VI) adsorption on the adsorbent. $C_0$=100 ppm, $m_{adsorbent}$=10 mg, t=60 min and T=298 K. (b) Effect of the contact time on the uranium(VI) adsorption on the adsorbent. $C_0$=100 ppm, $m_{adsorbent}$=10 mg, pH =2 and T=298 K.

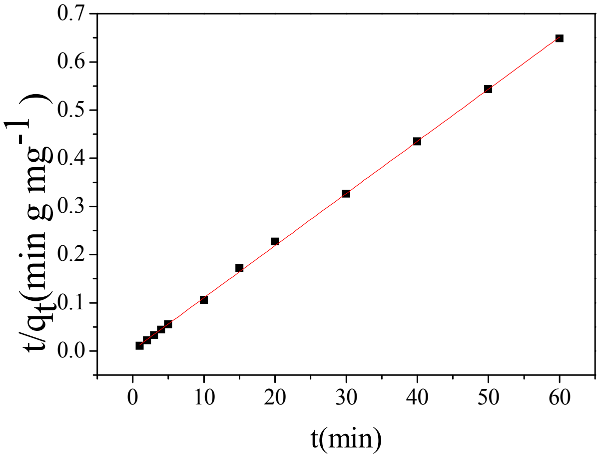

**Fig. 3** Pseudo second order fits for the kinetic date. $C_0$=100 ppm, $m_{adsorbent}$=10 mg, pH =2 and T=298 K.

So far, compared with a large number of reports on the adsorption capacity of adsorbents with high concentration uranium,[11,19,22] little attention has been paid to the rate of the adsorption; however, the adsorption rate is a key role for assessing the adsorbents in the practical application. For the sake of investigating the sorption rate of uranium(VI) onto this material, Fig. 2b shows the effect of the different contact time. It is notable that the adsorption equilibrium can be fast reached only within 1 min, which indicates very significant affinity between uranium(VI) and sorbent, possibly due to the coordination interactions between MOF and uranium(VI), as there exists abundant, free standing acylamide and carboxyl groups in the MOF channel and $UO_2^{2+}$ ions hold unique affinity towards oxygen atoms in nature. This can be further supported by the investigation of the kinetics of adsorption. The adsorption isotherm can be well fitted by the pseudo-second-order rate equation (2), see Fig. 3 and Table 1, implying a dominating chemic adsorption rather than physical adsorption in this system.

$$\frac{t}{q_t} = \frac{1}{k_2 q_e^2} + \frac{t}{q_e} \qquad (2)$$

**Table 1** Kinetic parameters for adsorption of $U^{2+}$

| T/K | pseudo-second order kinetics model | | |
|---|---|---|---|
| | $R^2$ | $k_2$(g·mg$^{-1}$min$^{-1}$) | $q_e$(mg·g$^{-1}$) |
| 298 | 0.999 | 0.0565 | 92.421 |

Note: $R^2$ is regression coefficient. $k_2$ (g·mg$^{-1}$· min$^{-1}$) denotes the adsorption rate constants of the pseudo-second-order adsorption. $q_t$ is the amounts of adsorption uranium adsorbed (mg/g) at the given time of ''t'', $q_e$ is the maximum adsorption capacity (mg/g).

The influence of temperature on adsorption was measured at 298K, 308K, 318K, giving that the adsorption capacity of uranium(VI) increases with the increase of the temperture, indicating that the process is endothermic in nature. Then the thermodynamics of adsorption is analyzed by using the following equations:

$$\ln K_d = \frac{\Delta S^{\circ}}{R} - \frac{\Delta H^{\circ}}{RT} \qquad (3)$$

$$\Delta G^{\circ} = \Delta H^{\circ} - T\Delta S^{\circ} \qquad (4)$$

$$K_d = \frac{q_e}{C_e} = \frac{(C_0 - C_e)}{C_e}\frac{V}{m} \qquad (5)$$

Where $K_d$ is the distribution coefficient (mL·g$^{-1}$) of U(VI), T is the absolute temperature (K) and R is the ideal gas constant (8.314 J/(mol K)). The values of $\Delta H^{\circ}$ (standard enthalpy change ) and $\Delta S^{\circ}$ (standrad entropy change) are calculated from the slope and intercept of the linear regression of lnKd versus 1/T (Fig. 4). The Gibbs free energy change ($\Delta G^{\circ}$) can be calculated by the equation (4). The values of thermodynamic parameters for the adsorption of uranium(VI) at different temperature were given in Table 2. The positive value of $\Delta H^{\circ}$ suggests that the sorption process of uranium (VI) is endothermic in nature. $\Delta G^{\circ}$is negative, which indicates the feasibility and spontaneity of the adsorption process.

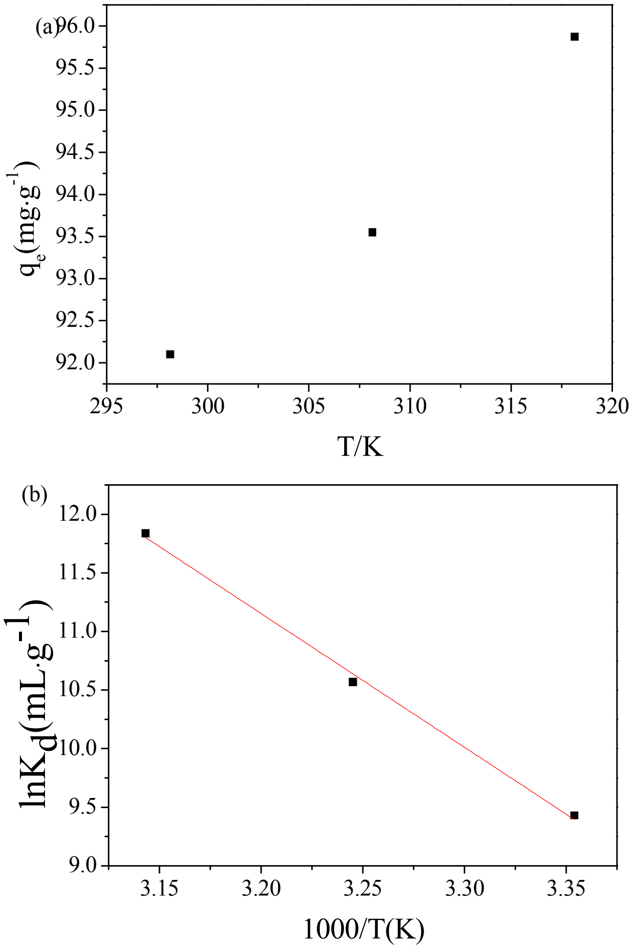

**Fig. 4** (a) The influence of temperature on the U(VI) sorption on the MOF; (b) Relationship curve between ln Kd and 1000/1T. $C_0$=100ppm, $m_{adsorbent}$=10mg, pH =2 and t=5 min.

**Table 2** The thermodynamic parameters of U(VI) adsorption

| $\Delta H^{\circ}$(kJ/mol) | $\Delta S^{\circ}$(J/(mol k)) | $\Delta G^{\circ}$(kJ/mol) | | |
|---|---|---|---|---|
| 94.9 | 396.5 | 298K | 308K | 318K |
| | | -23.3 | -27.2 | -31.2 |

To evaluate the maximum sorption capacity, the adsorption isotherm was measured, see Fig. 5. Langmuir and Freundlich equations are the most frequently used for describing adsorption isotherms. Generally speaking, the Langmuir model, which assumes that there is no interaction between the adsorbate molecules and the adsorption is localized in a monolayer, can be represented by the following equation (6), whereas the Freundlich model proposes an empirical model that is based on adsorption on heterogeneous surface and can be expressed as equation (7).

$$\frac{C_e}{q_e} = \frac{C_e}{q_m} + \frac{1}{k_l q_m} \qquad (6)$$

$$\ln q_e = \ln k_f + \frac{1}{n}\ln C_e \qquad (7)$$

Where $q_e$ is the amount adsorbed at equilibrium ($mg \cdot g^{-1}$) and $C_e$ is the equilibrium concentration ($mg \cdot L^{-1}$). $q_m$ is the maximum amount or the saturated adsorption amount ($mg \cdot g^{-1}$). $k_l$ is an equilibrium constant related to the binding strength ($L \cdot mg^{-1}$). n and $k_f$ are Freundlich constants which are indicators of the adsorption capacity and adsorption intensity, respectively.

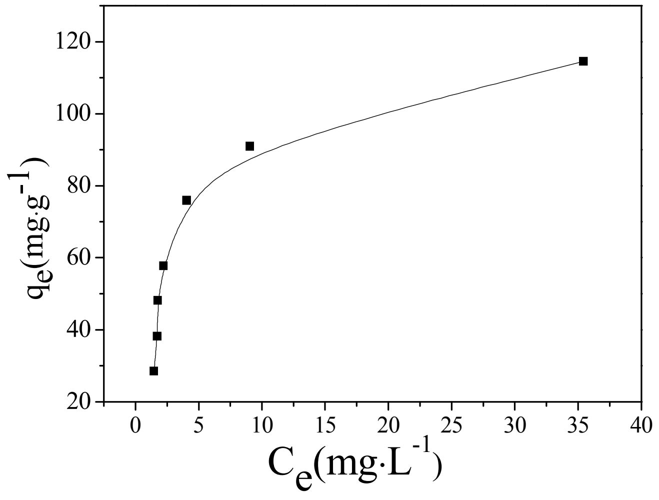

**Fig. 5** Adsorption isotherm of uranium ion on the MOF. $m_{adsorbent}$=10 mg, pH=2, t=5 min and T=298K.

**Table 3** Adsorption constants for Langmuir and Freundlich isotherm models

| T/K | Langmuir adsorption isotherm | | | Freundlich adsorption isotherm | | |
|---|---|---|---|---|---|---|
| 298 | $q_m$(mg/g) | $k_l$ | $R^2$ | $k_f$ | n | $R^2$ |
| | 125.944 | 0.289 | 0.994 | 46.247 | 3.649 | 0.899 |

The fitting results are listed in Table 3. It is clear that the Langmuir model is more appropriate than Freundlich model to depict the adsorption of uranium with a higher correlation coefficient ($R^2$) of 0.994, which indicates the adsorption is localized in a monolayer. In terms of the Langmuir equation the maximum adsorption capacity $q_e$ is estimated to be 125 mg/g, which is close to the experimental data of 115 mg/g.

For the practical application, the regeneration and reuse performance of adsorbent is of great significance. Then, the MOF sorbent after uranium uptake was digested by pure water, or 0.1 M HCl, or 0.1M $HNO_3$, or 0.1M $Na_2CO_3$ aqueous solutions, respectively. The elution efficiency of them is shown in Fig. 6 and Table 4. Notably, uranium(VI) ions could be almost completely desorbed when using 0.1M $Na_2CO_3$ eluant.[11] This high regeneration efficiency and easy separation from adsorption medium shows big potential in extraction of uranium from nuclear industry wastewater and seawater.

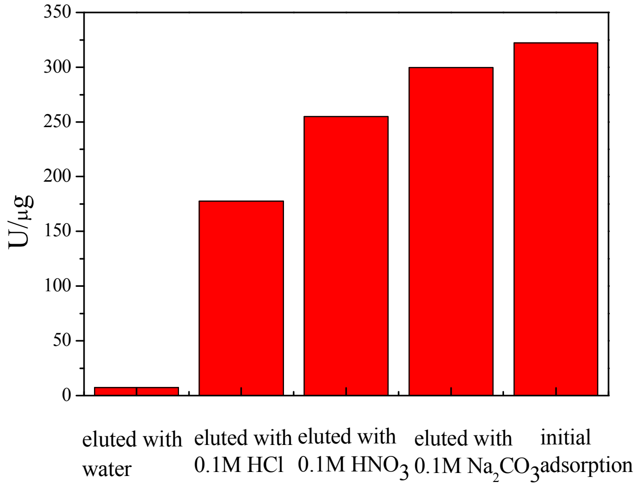

**Fig. 6** The elution efficiency upon different elution solution.

**Table 4** The elution efficiency for different eluant

| Eluent | elution efficiency |
|---|---|
| water | 2.2% |
| 0.1M HCl | 55.1% |
| 0.1M $HNO_3$ | 79.1% |
| 0.1M $Na_2CO_3$ | 93.0% |

According to the above research, we can make a conclusion that the MOF not only provides a rapid way for removing the suspension from aqueous solution, but also shows a very high release efficiency of uranium after the adsorption process, which could be a very promising material applying to the collection of uranium from seawater. Then, we explored extraction of uranium from seawater based on the present MOF material. Notably, within one minute in 1 L artifical seawater (pH=7.8) with the uranium(VI) concentration of 6 ppb,[23] the fresh MOF material (10 mg) will give an one-off extraction efficiency of 0.53 mg/g, where the eluant is 0.1M $Na_2CO_3$ aqueous solution, implying significant potential in extraction of uranium from seawater. Moreover, the regenerable adsorbent after $Na_2CO_3$ treatment is further utilized to extract uranium from seawater, giving the extraction efficiency of 0.51mg/g for the second time and 0.47 mg/g for the third time, indicating a regenerable property of this MOF material.

To confirm the chemic stability of the MOF material after extraction of uranium from seawater, we carried out the powder X-ray diffraction (PXRD) investigation, see Fig. 7. As attested by the excellent match of their PXRD patterns, high chemic stability of this MOF material even after extraction of uranium from seawater is observed. However, two obviously new peak appeared at high angle of 2θ=15.7° and 20.4°, mainly due to the formation a more dense phase as a result of the uptake of $UO^{2+}$ ions in the MOF channels. In addition, the chemic stability is further confirmed by filtration test, giving that the filtrate holds no obvious residue like that of organic ligand and Zn(II) ions, suggesting that part dissolution of MOF material in this system is excluded. Further, the surface morphology and chemic composition of the MOF sample material after full packing $UO^{2+}$ ions was characterized by SEM (Scanning Electron Microscope) and EDS (Energy Dispersive Spectrometer) investigation (Fig. 8, 9). The perfect hexagonal pillar-like crystals of as-synthesized samples are badly eroded after full packing $UO^{2+}$ ions. The content given by EDS spectra of U is 1.13%, close to Zn of 1.46%, approximately equal to adsorption amount of 76 mg/g, slightly less than the experimental and theoretical value, implying that the $UO^{2+}$ uptake is uneven for every MOF crystal and by contrast, the experimental and theoretical value is an average statistical result. According, based on the max adsorption amount of U(VI) and element analysis (C 47.93%, H 2.85%, N 6.82%) we can estimate the possible chemic formula, $[Zn(BTC)(L)][UO_2]_{0.5}\cdot(H_2O)_{1.5}$, for the $UO^{2+}$ loaded samples. Besides, TGA (thermogravimetric analysis) is also employed to trace the $UO^{2+}$ loaded samples, see Fig. 10. In contrast to the as-synthesized samples that shows major weight loss (14%) of solvent molecule at 40-290°C, the $UO^{2+}$ loaded samples loss solvent molecule at low temperature before 110°C only with a very small weigh loss (3.5%, equal to 1.5 water molecule of 3.3%), directly supporting the fact of $UO^{2+}$ loaded.

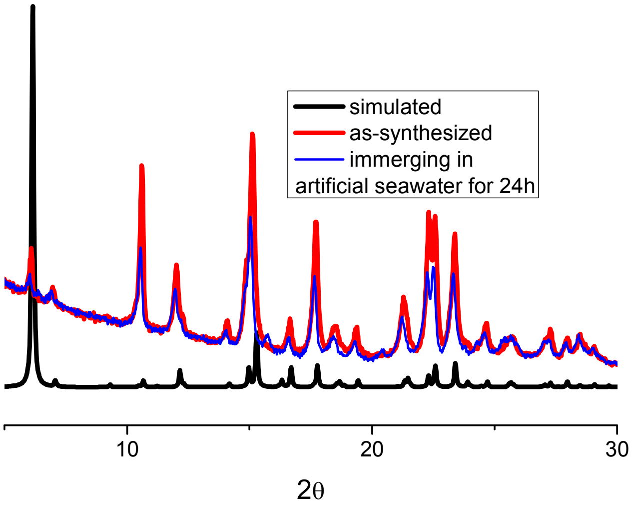

**Fig.7.** The PXRD patterns from simulated single crystal data, of as-synthesized samples, of as-synthesized samples after immerging in artificial seawater for 24 h.

To realize the adsorption mechanism in this system, IR (Infrared Spectroscopy) spectrum is carried out for as-synthesized samples and $UO^{2+}$ loaded samples (Fig. 11). The appearance of new peak at 935 $cm^{-1}$ is typical of characteristic stretching bond of $UO^{2+}$, confirming the fact of $UO^{2+}$ loaded, while another new peak at 740 $cm^{-1}$ implies the formation of additional U-O bond. For the as-synthesized samples, the free standing -COOH groups afford the characteristic IR bonds at 3297 and 1721 $cm^{-1}$, whereas such feature is absence and emergence of new peak at 1581 $cm^{-1}$ for the MOF materials after loading $UO^{2+}$ ions, suggesting the deprotonation of them and coordination interaction between carboxylate and $UO^{2+}$ ions. Moreover, the shift of the characteristic C=O stretching bond from 1687 $cm^{-1}$ to 1694 $cm^{-1}$ for acylamide group is possibly due to U→O contact between $UO^{2+}$ ions and C=O unit.

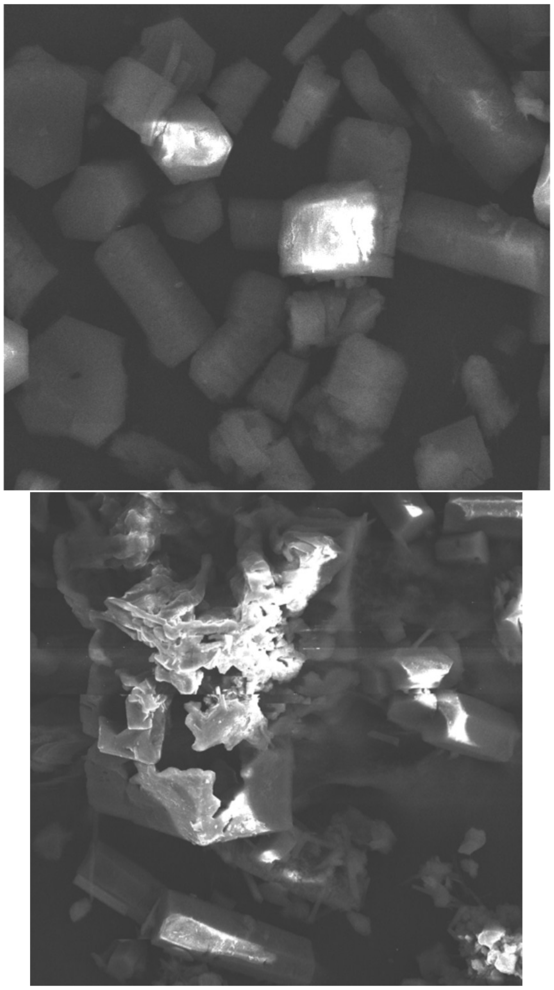

**Fig. 8** SEM image of as-synthesized samples and samples after loading U(VI).

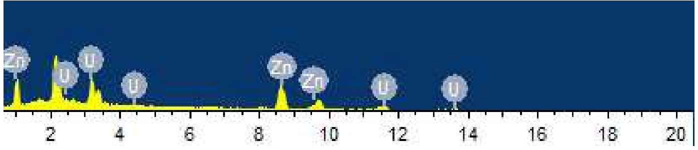

**Fig. 9** EDS spectra of the as-synthesized samples after loading U(VI).

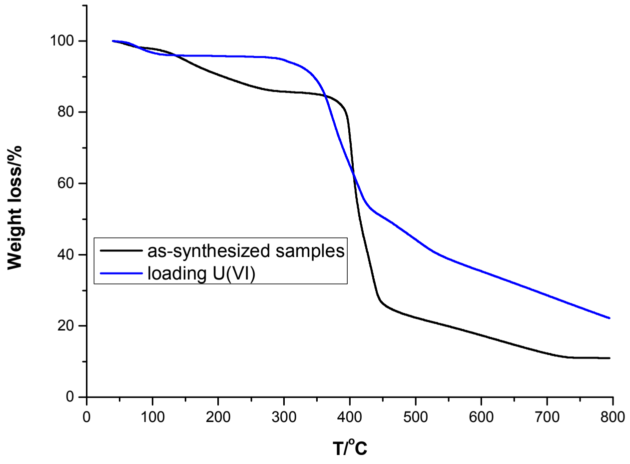

**Fig. 10** The TG plots of as-synthesized samples and the samples after loading U(VI).

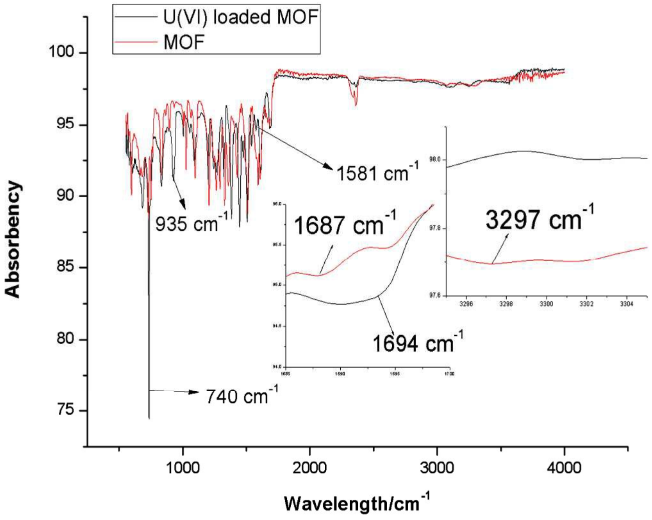

**Fig. 11** The IR spectrum of both U(VI) loaded samples and as-synthesized samples.

For MOFs used in the U(VI) adsorption, there were two outstanding reports by Lin[18] and Sun[11]. Lin *et al* used modified UiO-68 and generated a 217 mg/g U(VI) adsorption capability, while based on **MOF-76** Sun *et al* obtained a 298 mg/g U(VI) adsorption capability, where Lin *et al* suggested an adsorption mechanism based on the coordination interactions between phosphorylurea ligand and U(VI) ions, whereas Sun *et al* suggested interactions between MOF skeleton and U(VI) ions that should be responsible for the excellent U(VI) adsorption capability. Moreover, their adsorption equilibrium times were estimated to be 1h and 5h, respectively. Moreover, Lin *et al* also explored adsorption of U(VI) from artifical seawater, but the U(VI) content is 100 ppm rather than 1-7 ppb in the actual seawater. As we know, most of materials hold excellent U(VI) adsorption capability under high U(VI) concentration in the magnitude of ppm and afford almost no adsorption of U(VI) in the magnitude of ppb.[22] By contrast, the smaller U(VI) adsorption capability of 115 mg/g observed for the present MOF is mainly due to the smaller aperture of this MOF. However, due to the existence of extensive free standing carboxyl and acylamide groups this MOF material performs a fast adsorption equilibrium within one minute and an outstanding U(VI) extraction from artifical seawater (U(VI) in the magnitude of ppb) with extraction efficiency of 0.53 mg/g. Furthermore, MOF material without any pretreatment for U(VI) adsorption seems unique for the present MOF.

## Conclusion

In summary, this study systematically evaluates a MOF material with the pore wall functionalized by both carboxyl groups and acylamide groups towards the extraction of $UO^{2+}$ ions from water in detail and a facile approach has been successfully achieved. Notably, without any pre-treatment and with 1 min, this MOF material shows excellent ability of high-performance extraction (115 mg $g^{-1}$) at low pH, thus preforming a big potential in the extraction of $UO^{2+}$ ions from water. This is mainly driven by the coordination interactions between $UO^{2+}$ ions and free standing carboxyl groups in the MOF channel, and consequently a chemic adsorption. Importantly, ultra-fast, high-performance, and no pretreatment extraction of $UO^{2+}$ ions from simulated seawater is also observed. As a result, an one-off extraction efficiency of 0.53 mg/g can be obtained from 1L artificial seawater in the concentration of 6 ppb, suggesting significant and promising potential in extraction of $UO^{2+}$ ions from seawater. In this regard, more elaborate designs are currently underway to improve the extraction ability of this technique, while maintaining the simplicity and efficiency of preparation and application.

## Acknowledgements

This work was supported by the NSF of China (21203022, 21261001, 21361001), the Natural Science Foundation of Jiangxi Province of China (no. 20143ACB20002, 20151BAB203001), and the Young scientist training program of Jiangxi Province of China (no. 20142BCB23018), and the graduate innovation project of East China Institute of Technology (DHYC2014022).

## Notes and references

College of Biology, Chemistry and Material Science, East China Institute of Technology, Fuzhou, Jiangxi 344000, P. R. China, ecitluofeng@163.com

1 (a) G. T. Rochelle, *Science* 2009, **325**, 1652; (b) J. Liu, P. K. Thallapally, B. P. McGrail, D. R. Brown, J. Liu, *Chem. Soc. Rev.*, 2012, **41**, 2308; (c) K. Sumida, D. L. Rogow, J. A. Mason, T. M. McDonald, E. D. Bloch, Z. R. Herm, T. H. Bae, J. R. Long, *Chem. Rev.* 2012, **112**, 724; (d) A. H. Lu, G. P. Hao, *Annu. Rep. Prog. Chem., Sect. A: Inorg. Chem.*, 2013, **109**, 484.
2 K. K. Tanabe, S. M. Cohen, *Chem. Soc. Rev.* 2011, **40**, 498.
3 D. H. Liu, C. L. Zhong, *J. Mater. Chem.* 2010, **20**, 10308.
4 (a) Z. J. Lin, J. Lu, M. C. Hong, R. Cao, *Chem. Soc. Rev.* 2014, **43**, 5867; (b) X. L. Wu, F. Luo, G. M. Sun, A. M. Zheng, J. Zhang, M. B. Luo, W. Y. Xu, Y. Zhu, X. M. Zhang, S. Y. Huang, *ChemPhysChem.* 2013, **14**, 3594; (c) Y. C. Qin, X. F. Feng, F. Luo, G. M. Sun, Y. M. Song, X. Z. Tian, H. X. Huang, Y. Zhu, Z. Z. Yuan, M. B. Luo, S. J. Liu, W. Y. Xu, *Dalton Trans.* 2013, **42**, 50; (d) F. Luo, C. B. Fan, M. B. Luo, X. L. Wu, Y. Zhu, S. Z. Pu, W. Y. Xu, G. C. Guo, *Angew. Chem. Int. Ed.* 2014, **53**, 9298.

5 (a) R. C. Huxford, J. D. Rocca, W. B. Lin, C. Opin, *Chem. Biol.* **2010**, *14*, 262; (b) F. Luo, S. R. Batten, *Dalton Trans.* 2010, **39**, 4485.

6 D. M. DAlessandro, B. Smit, J. R. Long, *Angew. Chem. Int. Ed.* 2010, **49**, 6058.

7 Q. L. Zhu, C. J. Shen, C. H. Tan, T. L. Sheng, S. M. Hu, X. T. Wu, *Chem. Commun.* 2012, **48**, 531.

8 M. Kurmoo, *Chem. Soc. Rev.*2009, **38**, 1353.

9 H. R. Moon, D. W. Lim, M. P. Suh, *Chem. Soc. Rev.* 2013, **42**, 1807.

10 Y. Basdogan, S. Keskin, *CrystEngComm.* 2015, **17,** 261.

11 W. T. Yang, Z. Q. Bai, W. Q. Shi, L. Y. Yuan, T. Tian, Z. F. Chai, H. Wang, Z. M. Sun, *Chem. Commun.* 2013, **49**, 10415.

12 K. Margarete, W. N. Wheeler, G. Meinrath, *J. Environ. Radioactiv.* 2005, **78**, 151.

13 Annual Report 2011. International Atomic Energy Agency, Vienna.

14 H. J. Zhang, H. L. Liang, Q. D. Chen, X. H. Shen, *J. Radioanal. Nucl. Chem.* 2013, **298**, 1705.

15 Y. F. Yue, X. G. Sun, R. T. Mayes, J. S. Kim, P. F. Fulvio, Z. A. Qiao, S. Brown, S. Dai, *Sci. China Chem.* 2013, **56**, 1510.

16 X. F. Zhang, J. Wang, R. M. Li, Q. H. Dai, L. H. Liu, *New J. Chem.* 2013, **37**, 3914.

17 L. Q. Ma, C. Abney, W. B. Lin, *Chem. Sov. Rev.* 2009, **38**, 1248.

18 M. Carboni, C. W. Abney, S. B. Liu, W. B. Lin, *Chem. Sci.* 2013, **4**, 2396.

19 F. Luo, M. S. Wang, M. B. Luo, G. M. Sun, Y. M. Song, P. X. Li, G. C. Guo, *Chem. Commun.* 2012, **48**, 5989.

20 (a) Y. Belmabkhout, H. Mouttaki, J. F. Eubank, V. Guillerm, M. Eddaoudi, *RSC Adv.,* 2014, **4**, 63855; (b) F. Ragon, B. Campo, Q. Y. Yang, C. Martineau, A. D. Wiersum, A. Lago, V. Guillerm, C. Hemsley, J. F. Eubank, M. Vishnuvarthan, F. Taulelle, P. Horcajada, A. Vimont, P. L. Llewellyn, M. Daturi, S. Devautour-Vinot, G. Maurin, C. Serre, T. Devic, G. Clet, *J. Mater. Chem. A*, 2015, **3**, 3294.

21 H. A. Rossiter, M. Graham, A. Schafer, *Sep. Purif. Technol.* 2010, **71**, 89.

22 (a) M. J. Manos, M. G. Kanatzidis, *J. Am. Chem. Soc.* 2012, **134**, 16441; (b) S. L. Ma, L. Huang, L. J. Ma, Y. Shim, S. M. Islam, P. L. Wang, L. D. Zhao, S. C. Wang, G. B. Sun, X. J. Yang, M. G. Kanatzidis, *J. Am. Chem. Soc.* 2014, in press, doi: 10.1021/jacs. 5b00762.

23 K. Saito, T. Miyauchi, *J. Nucl. Sci. Technol.* 1982, **19**, 145.